

# Hydrolytic and Enzymatic Degradation of Nanoparticles Based on Amphiphilic Poly( $\gamma$ -glutamic acid)-*graft*-L-Phenylalanine Copolymers

Takami Akagi,<sup>†,‡</sup> Mariko Higashi,<sup>†,‡</sup> Tatsuo Kaneko,<sup>†,‡</sup> Toshiyuki Kida,<sup>†,‡</sup> and Mitsuru Akashi<sup>\*,†,‡</sup>

Department of Applied Chemistry, Graduate School of Engineering, Osaka University, 2-1 Yamadaoka, Suita 565-0871, Japan, and Core Research for Evolutional Science and Technology (CREST), Japan Science and Technology Agency (JST), Tokyo, Japan

Received September 8, 2005; Revised Manuscript Received November 8, 2005

Amphiphilic graft copolymers consisting of poly( $\gamma$ -glutamic acid) ( $\gamma$ -PGA) as the hydrophilic backbone and L-phenylalanine ethylester (L-PAE) as the hydrophobic side chain were synthesized by grafting L-PAE to  $\gamma$ -PGA. The nanoparticles were prepared by a precipitation method, and about 200 nm-sized nanoparticles were obtained due to their amphiphilic properties. The hydrolytic and enzymatic degradation of these  $\gamma$ -PGA nanoparticles was studied by gel permeation chromatography (GPC), scanning electron microscopy (SEM), dynamic light scattering (DLS) and <sup>1</sup>H NMR measurements. The hydrolysis ratio of  $\gamma$ -PGA and these hydrophobic derivatives was found to decrease upon increasing the hydrophobicity of the  $\gamma$ -PGA derivatives. The pH had an effect on the hydrolytic degradation of the polymer. The hydrolysis of the polymer could be accelerated by alkaline conditions. The degradation of the  $\gamma$ -PGA backbone by  $\gamma$ -glutamyl transpeptidase ( $\gamma$ -GTP) resulted in a dramatic change in nanoparticle morphology. With increasing time, the  $\gamma$ -PGA nanoparticles began to decrease in size and finally disappeared completely. Moreover, the  $\gamma$ -PGA nanoparticles were degraded by four different enzymes (Pronase E, protease, cathepsin B and lipase) with different degradation patterns. The enzymatic degradation of the nanoparticles occurred via the hydrolysis of  $\gamma$ -PGA as the main chain and L-PAE as the side chain. In the case of the enzymatic degradation of  $\gamma$ -PGA nanoparticles with Pronase E, the size of the nanoparticles increased during the initial degradation stage and decreased gradually when the degradation time was extended. Nanoparticles composed of biodegradable amphiphilic  $\gamma$ -PGA with reactive function groups can undergo further modification and are expected to have a variety of potential pharmaceutical and biomedical applications, such as drug and vaccine carriers.

## Introduction

Biodegradable polymeric nanoparticles have been widely used in biomedical applications, such as drug, gene, and vaccine delivery systems.<sup>1</sup> Amphiphilic block or graft copolymers consisting of hydrophilic and hydrophobic segments are self-assembling materials and are capable of forming polymeric associates in aqueous solutions. Aggregates of various morphologies have been observed in a number of self-assembled polymeric systems. The morphology of the nanoparticles produced from amphiphilic block/graft copolymers can be varied by changing the composition of the hydrophobic and hydrophilic blocks on the polymer chains.<sup>2–4</sup> Recently, many studies have focused on self-assembled biodegradable nanoparticles for biomedical and pharmaceutical applications. The commonly used biodegradable polymers are aliphatic polyesters, such as poly(lactic acid) (PLA), poly(glycolic acid) (PGA), poly( $\epsilon$ -caprolactone) (PCL), and their copolymers.<sup>5,6</sup> Amphiphilic block copolymers such as poly(ethylene glycol)-*b*-poly(lactic acid) (PEG-*b*-PLA), or PEG-*b*-PCL, are very attractive for use as drug delivery applications.<sup>7–12</sup> Hydrophobic blocks form the inner core of the structure, which acts as an incorporation site for

therapeutic agents, especially for hydrophobic drugs. However, an important limitation in the use of these polyesters for biomedical applications is their lack of reactive functional groups to which biomolecules or drugs can be covalently immobilized.

The biodegradation rate and the release kinetics of loaded drugs can be controlled by their composition ratio and the molecular weight of the polymer and graft or block copolymers.<sup>13–16</sup> Therefore, a study of the degradation kinetics is important for biodegradable polymers. However, the degradation properties of nanoparticles prepared from amphiphilic polymers have been studied only by a few research groups. Wu et al. reported a study on the enzymatic degradation behavior of PEG-*b*-PCL and PCL-*b*-PEG-*b*-PCL nanoparticles using laser light scattering.<sup>17–19</sup> The degradation of these copolymer micelles in the presence of lipase was much faster than bulk PCL or PCL thin film. Moreover, Tom et al. studied the hydrolytic degradation of Pluronic F127/PLA block copolymer nanoparticles using various physical techniques.<sup>20,21</sup> It was reported that the hydrolytic degradation of the amphiphilic block copolymers affected their particle size and morphologies.

We previously reported that core-corona polymeric nanoparticles composed of hydrophobic polystyrene and hydrophilic macromonomers could be prepared by free radical dispersion copolymerization.<sup>22,23</sup> Core-corona type polymeric nanoparticles have applications in various technological and biomedical fields, because their chemical structures can be easily controlled.

\* To whom correspondence should be addressed. Tel: +81-6-6879-7356. Fax: +81-6-6879-7359. E-mail: akashi@chem.eng.osaka-u.ac.jp.

<sup>†</sup> Osaka University.

<sup>‡</sup> CREST.

**Table 1.** Synthesis of  $\gamma$ -PGA-graft-L-PAE Copolymers

| sample                       | $\gamma$ -PGA<br>(unit mmol) | L-PAE<br>(mmol) | WSC<br>(mmol) | yield<br>(%) | grafting<br>degree<br>(%) <sup>a</sup> | particle<br>size (nm) <sup>b</sup> | zeta potential<br>(mV) <sup>c</sup> |
|------------------------------|------------------------------|-----------------|---------------|--------------|--|------------------------------------|-------------------------------------|
| $\gamma$ -PGA-graft-L-PAE-10 | 4.7                          | 4.7             | 0.47          | 50           | 10                                     | no particles                       |                                     |
| $\gamma$ -PGA NP-53          | 4.7                          | 4.7             | 4.7           | 65           | 53                                     | 200                                | -23.8                               |
| $\gamma$ -PGA NP-74          | 4.7                          | 11.6            | 4.7           | 78           | 74                                     | 183                                | -25.0                               |

<sup>a</sup> The degree of grafting of L-PAE was measured by <sup>1</sup>H NMR. <sup>b</sup> The particle size of the  $\gamma$ -PGA nanoparticles was measured in PBS by dynamic light scattering. <sup>c</sup> The zeta potential of the  $\gamma$ -PGA nanoparticles was measured in PBS using a Zetasizer nano ZS.

These nanoparticles have been utilized as controlled-release carriers for peptide drugs physically adsorbed onto their surfaces.<sup>24</sup> Moreover, lectin-immobilized nanoparticles can efficiently capture human immunodeficiency virus type 1 (HIV-1) via the mannose residues of gp120.<sup>25</sup> These HIV-1-capturing nanoparticles were utilized as nanoparticle-based vaccine carriers and were useful as carriers for a prophylactic vaccine against HIV-1 infection.<sup>26–29</sup> However, both biodegradability and biocompatibility are required for medical use. Therefore, the development of biodegradable nanoparticles is indispensable for these applications.

In a previous study, we prepared nanoparticles composed of hydrophobically modified poly( $\gamma$ -glutamic acid) ( $\gamma$ -PGA).<sup>30–32</sup> These  $\gamma$ -PGA nanoparticles showed great potential as carriers as a protein delivery system, and the nanoparticles did not induce any cytotoxicity.<sup>33</sup>  $\gamma$ -PGA is composed of naturally occurring D- and L-glutamic acid linked together through amide bonds. The  $\alpha$ -carboxylate side chains of  $\gamma$ -PGA can be chemically substituted to introduce various bioactive ligands or to modulate the overall hydrophobicity of the polymer. We have also developed a modified method to prepare  $\gamma$ -PGA as a drug delivery carrier,<sup>34</sup> as a tissue engineering material<sup>35</sup> and as a thermosensitive polymer.<sup>36</sup> In this study, we prepared nanoparticles from amphiphilic  $\gamma$ -PGA derivatives conjugated with an L-phenylalanine ethylester (L-PAE) to study their hydrolytic and enzymatic degradation behavior. The degradation behavior of these nanoparticles was investigated by GPC, SEM, DLS, and <sup>1</sup>H NMR. We examined the enzymatic degradation of these  $\gamma$ -PGA nanoparticles by  $\gamma$ -glutamyl transpeptidase ( $\gamma$ -GTP) and protease.  $\gamma$ -GTP is found widely from bacteria to animals, and catalyzes the hydrolysis and transpeptidation of  $\gamma$ -glutamyl compounds and the transfer of their glutamyl moieties to amino acids and peptides. The detection of degradation products from the enzymatic degradation of  $\gamma$ -PGA nanoparticles was also investigated by ninhydrin assay.

## Experimental Section

**Materials.**  $\gamma$ -PGA ( $M_w$  = 300 000) was kindly donated by Meiji Seika Co. Ltd. L-phenylalanine ethylester (L-PAE), poly(L-glutamic acid) ( $\alpha$ -PGA) ( $M_w$  = 100 000),  $\gamma$ -glutamyl transpeptidase ( $\gamma$ -GTP) from bovine kidney (2.9 units/mg), Pronase E from *Streptomyces grisei* (4.4 units/mg), protease from *Aspergillus sojae* (0.3 units/mg), cathepsin B from bovine spleen (5.6 units/mg) and lipase from porcine pancreas (30 units/mg) were purchased from Sigma (St. Louis MO). 1-Ethyl-3-(3-dimethylaminopropyl) carbodiimide (water-soluble carbodiimide, WSC), dimethyl sulfoxide (DMSO), dimethyl formamide (DMF), glycine, and glycyglycine were purchased from Wako Pure Chemical Industries (Osaka, Japan).

**Synthesis of  $\gamma$ -PGA-graft-L-PAE and Preparation of  $\gamma$ -PGA Nanoparticles.** The  $\gamma$ -PGA-graft-L-PAE copolymers were synthesized as previously described.<sup>30</sup> Briefly,  $\gamma$ -PGA (4.7 unit mmol) was hydrophobically modified by L-PAE in the presence of WSC for 24 h at room temperature. Different amounts of WSC (0.47 and 4.7 mmol) and L-PAE (4.7 and 11.6 mmol) per glutamic acid residue of  $\gamma$ -PGA

were then added (Table 1). The purified  $\gamma$ -PGA-graft-L-PAE was characterized by <sup>1</sup>H NMR and FT-IR spectroscopy to determine the degree of L-PAE grafting. The degree of grafting of L-PAE was controlled by altering the amount of WSC and L-PAE. In this experiment,  $\gamma$ -PGA-graft-L-PAE with 10, 53, and 74% grafting degrees was used. Nanoparticles composed of  $\gamma$ -PGA-graft-L-PAE were prepared by a precipitation and dialysis method. First, the  $\gamma$ -PGA-graft-L-PAE (10 mg) was dissolved in 1 mL of DMSO, and water at the same volume was added to yield a translucent solution. The solution was then dialyzed for 72 h against distilled water to form the nanoparticles. The  $\gamma$ -PGA-graft-L-PAE copolymers were not degraded under these conditions. The dialyzed solutions obtained were then freeze-dried.

**Particle Size and Zeta Potential Measurements.** The particle size distribution of the  $\gamma$ -PGA nanoparticles in aqueous solution was measured by a dynamic light scattering (DLS) method using a Zetasizer Nano ZS (Malvern Instruments, U.K.). The surface charge of the  $\gamma$ -PGA nanoparticles was determined by zeta potential measurement using a Zetasizer Nano ZS. The nanoparticle suspension was diluted with PBS (0.1 mg/mL) and was used for both particle size and zeta potential measurements without filtering.

**Hydrolytic Degradation.**  $\gamma$ -PGA,  $\gamma$ -PGA-graft-L-PAE-10 (grafting degree: 10 L-PAE groups per 100 glutamic acid units of  $\gamma$ -PGA, 10% graft copolymers dissolved in aqueous solution), and nanoparticles (NP) composed of  $\gamma$ -PGA-graft-L-PAE-53 ( $\gamma$ -PGA NP-53) were dissolved or dispersed in 0.2 M phosphate buffer (PB) (pH 7.4) or Na<sub>2</sub>HPO<sub>4</sub>/NaOH buffer (pH 12), respectively. Three samples (1.25 mg/mL) were then incubated in an aluminum block bath at 80 °C. At predetermined intervals, degradation samples of  $\gamma$ -PGA and  $\gamma$ -PGA-graft-L-PAE-10 were withdrawn and filtered and the molecular weights measured by gel permeation chromatography (GPC) (TSK-GEL G4000PW<sub>XL</sub> column). The degradation samples of  $\gamma$ -PGA NP-53 were dried and dissolved in DMF for the GPC measurements (TSK-GEL SuperH4000 column), and insoluble inorganic salts were filtered before the GPC measurement. About 5 mg of the sample was dissolved in 1 mL of DMF, and injection volumes of 200  $\mu$ L were used. The GPC system used 0.2 M PB (pH 7.4), Na<sub>2</sub>HPO<sub>4</sub>/NaOH buffer (pH 12), and DMF as the mobile phase, with a flow rate of 1 mL/min. Calibration was performed with poly(ethylene glycol) (PEG) and polystyrene standards. The degradation ratio was calculated based on the shift of the main polymeric peak with time and was expressed as a percentage of degradation. The degradation ratio was calculated as:  $[(M_{n0} - M_{nt})/M_{n0}] \times 100$ , where  $M_{n0}$  and  $M_{nt}$  are the number-averaged molecular weight prior to degradation and the  $M_n$  at "t" time of degradation, respectively.

**Enzymatic Degradation of  $\gamma$ -PGA Nanoparticles.** Five enzymes ( $\gamma$ -GTP, Pronase E, protease, cathepsin B and lipase) were used for the enzymatic degradation.  $\gamma$ -PGA,  $\gamma$ -PGA NP-53,  $\gamma$ -PGA-graft-L-PAE-74 ( $\gamma$ -PGA NP-74), and  $\alpha$ -PGA (1.25 mg/mL) were incubated in 50 mM PB (pH 8.0) containing 2.9 units/mL of  $\gamma$ -GTP and 50 mM glycyglycine at 37 °C in a water bath.  $\gamma$ -PGA,  $\gamma$ -PGA NP-53, and  $\alpha$ -PGA (1.25 mg/mL) were incubated in pH 7.4, 7.4, 6.5, and 7.2 (50 mM PB) for Pronase E, protease, cathepsin B, and lipase, respectively. The reaction mixture consisting of 10 units/mL of each enzyme was then incubated for various times at 37 °C. At predetermined time intervals, samples were withdrawn and freeze-dried. The molecular weights were measured by GPC as described above.

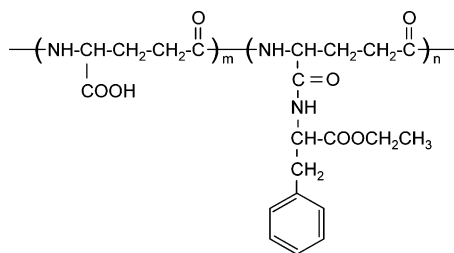


Figure 1. Chemical structure of  $\gamma$ -PGA-*g*-L-PAE.

**Scanning Electron Microscope (SEM) Measurements.** The degradability of the  $\gamma$ -PGA nanoparticles with the enzyme was estimated by the morphological changes and particle size of the nanoparticles. The morphologies of the  $\gamma$ -PGA nanoparticles were observed by SEM (JSM-6700F, JEOL) at 20 kV. A drop of the nanoparticle suspension was placed on a glass surface, which was fixed on metallic supports with carbon tape. After drying, the samples were coated with osmic acid.

**Detection of Degradation Products from the Enzymatic Degradation of  $\gamma$ -PGA Nanoparticles.** The amount of degraded amino acids from the  $\gamma$ -PGA nanoparticles was determined by the ninhydrin assay. The enzymatic degradation samples were heated at 100 °C for 20 min following the addition of 0.5% (w/v) ninhydrin, 0.075% (w/v) hydrindantin, 20% (v/v) 2-methoxyethanol, and 0.25 M sodium acetate (pH 5.5). The developed color intensity was then measured with a microplate reader at 570 nm. Using a calibration curve for reference L-glutamic acid or L-PAE standards, the amount of degraded amino acids was determined. The degradation ratio was calculated as [(degraded amount of amino acids)/(initial feeding amount of polymer)]  $\times$  100. In addition, after the enzymatic degradation of the  $\gamma$ -PGA nanoparticles, the enzymes were inactivated by heat treatment for 5 min at 100 °C, and the samples were then dialyzed against distilled water using cellulose membrane tubing (50 000 molecular weight cut off) for 72 h at room temperature. The dialyzed solutions obtained were then freeze-dried and dissolved in DMSO- $d_6$  for the  $^1\text{H}$  NMR measurements.

## Results and Discussion

**Synthesis of  $\gamma$ -PGA-*g*-L-PAE and Preparation of  $\gamma$ -PGA Nanoparticles.** Amphiphilic  $\gamma$ -PGA was synthesized by the conjugation of L-PAE as the hydrophobic groups (Figure 1). Graft copolymers with different degrees of L-PAE grafting were prepared by changing the molar ratio of the glutamic acid units of  $\gamma$ -PGA and WSC or L-PAE (Table 1). Amphiphilic block/graft copolymers can self-aggregate in aqueous solution, due to their intra- and/or intermolecular hydrophobic interactions.<sup>37–40</sup> The  $\gamma$ -PGA nanoparticles were prepared by a precipitation and dialysis method. The  $\gamma$ -PGA-*g*-L-PAE could form nanoparticles due to its amphiphilic characteristics. These nanoparticles could be prepared from  $\gamma$ -PGA-*g*-L-PAE with 53 and 74% L-PAE grafting. However,  $\gamma$ -PGA-*g*-L-PAE-10 could not form nanoparticles due to the weak interactions between the L-PAE groups attached to the  $\gamma$ -PGA backbone. The specific self-assembly behavior of  $\gamma$ -PGA-*g*-L-PAE in aqueous solutions is due to multiple phenyl groups stacking. In our previous study,  $\gamma$ -PGA-*g*-leucine could not form stable nanoparticles.<sup>30</sup> These results suggested that the stacking effect of the phenyl groups is important for the stable formation of nanoparticles. The size distribution and surface charge of the  $\gamma$ -PGA nanoparticles in aqueous media were measured by DLS and zeta potential measurements. In these experiments, the particle size of the  $\gamma$ -PGA nanoparticles was about 200 nm and showed a highly negative zeta potential in PBS (Table 1). This negative charge of the  $\gamma$ -PGA nanoparticle surfaces is due to the carboxyl groups of  $\gamma$ -PGA. The structure

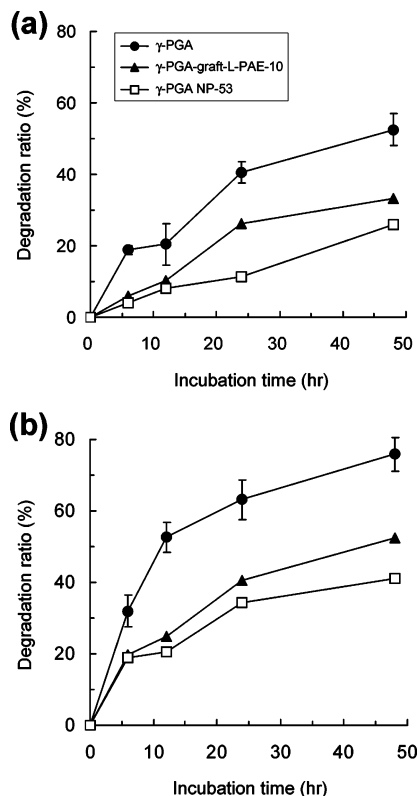


Figure 2. Degradation of  $\gamma$ -PGA and its derivatives by hydrolysis for different incubation periods in pH 7.4 (a) and pH 12 (b) at 80 °C. (●) Unmodified  $\gamma$ -PGA, (▲)  $\gamma$ -PGA-*g*-L-PAE-10 and (□)  $\gamma$ -PGA nanoparticles (NP) composed of  $\gamma$ -PGA-*g*-L-PAE-53 ( $\gamma$ -PGA NP-53). The degradation ratio was calculated as  $[(M_{n0} - M_{nt})/M_{n0}] \times 100$ , where  $M_{n0}$  and  $M_{nt}$  are the number-averaged molecular weight prior to degradation and the  $M_n$  at “t” time of degradation, respectively. The results for  $\gamma$ -PGA are presented as means  $\pm$  SD ( $n = 3$ ). The other results represent the average mean from two separate experiments.

of the nanoparticles is a core-shell type with a L-PAE core and an outer  $\gamma$ -PGA shell. However, unlike amphiphilic block copolymers, these  $\gamma$ -PGA-*g*-L-PAE copolymers have a very short hydrophobic domain. Therefore, it is suggested that the core of the nanoparticle is formed not only by L-PAE, but also by the  $\gamma$ -PGA of the main chain. Their hydrophilic domains are either exposed to the aqueous solvent or to a low level of hydrophilic domains present within the nanoparticles.

**Hydrolytic Degradation Behavior of  $\gamma$ -PGA Nanoparticles.** The biodegradability of the  $\gamma$ -PGA and  $\gamma$ -PGA nanoparticles was estimated from the decrease in their molecular weight following hydrolytic degradation. The hydrolysis of  $\gamma$ -PGA has been investigated in detail. Fan et al. investigated the hydrolysis of  $\gamma$ -PGA in different pH solutions.<sup>41</sup> When  $\gamma$ -PGA was incubated in a neutral buffer at 37 °C, only approximately 10% of the polymer had been hydrolyzed by 60 days. Goto et al. have also reported the effect of temperature on the hydrolysis of  $\gamma$ -PGA.<sup>42</sup> The rate of hydrolysis could be accelerated with an increase in temperature.

In this study, the hydrolysis of  $\gamma$ -PGA,  $\gamma$ -PGA-*g*-L-PAE-10, and  $\gamma$ -PGA-NP-53 was carried out at 80 °C in PB (pH 7.4 and 12) as an acceleration test. Three samples with different hydrophobicities were used to study the effect of the hydrophobicity of the polymer on the hydrolytic degradation behavior. After 6, 12, 24, and 48 h, the degraded samples of  $\gamma$ -PGA and its derivatives were analyzed using GPC. Figure 2 shows the increase in the degradation ratio versus the hydrolysis time at pH 7.4 (a) and 12 (b). An increase in the hydrolysis ratio was



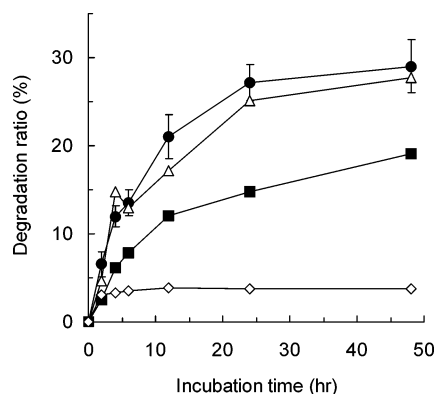


**Figure 3.** Degradation of  $\gamma$ -PGA,  $\gamma$ -PGA nanoparticles and  $\alpha$ -PGA by  $\gamma$ -GTP for different incubation periods at 37 °C. (●) Unmodified  $\gamma$ -PGA, ( $\Delta$ )  $\gamma$ -PGA-graft-L-PAE-53 ( $\gamma$ -PGA NP-53), (■)  $\gamma$ -PGA-graft-L-PAE-74 ( $\gamma$ -PGA NP-74) and ( $\diamond$ )  $\alpha$ -PGA. The degradation ratio was calculated as  $[(M_{n0} - M_{nt})/M_{n0}] \times 100$ , where  $M_{n0}$  and  $M_{nt}$  are the number-averaged molecular weight prior to degradation and the  $M_n$  at "t" time of degradation, respectively. The results for  $\gamma$ -PGA are presented as means  $\pm$  SD ( $n = 3$ ). The other results represent the average mean from two separate experiments.

observed for the three polymers, at both pH values. The hydrolysis profiles of  $\gamma$ -PGA and  $\gamma$ -PGA derivatives at pH 7.4 were found to be different based on the degree of grafting of L-PAE. After 48 h, the hydrolysis ratios were 53%, 33%, and 26% for  $\gamma$ -PGA,  $\gamma$ -PGA-graft-L-PAE-10, and  $\gamma$ -PGA-NP-53, respectively. The polymer hydrolysis profiles in pH 12 showed a same tendency for that of hydrolysis at pH 7.4. However, the polymer hydrolysis ratio was higher at pH 12 as compared to pH 7.4. This result suggested that the pH was an important factor for the degradation behavior of  $\gamma$ -PGA and its derivatives. Kubota et al. reported the alkaline hydrolysis of  $\gamma$ -PGA.<sup>43</sup> The hydrolysis of  $\gamma$ -PGA was accelerated by the addition of NaOH. The introduction of L-PAE into  $\gamma$ -PGA influenced the hydrolysis ratio of the polymer. The hydrolysis ratios of hydrophobically modified  $\gamma$ -PGA were much lower than that of unmodified  $\gamma$ -PGA, at both pH values. Furthermore, the hydrolysis ratio of  $\gamma$ -PGA-NP-53 was lower than those of  $\gamma$ -PGA-graft-L-PAE-10. These results indicated that the introduction of L-PAE groups into  $\gamma$ -PGA delayed the polymer hydrolysis. This could be attributed to the hydrophobicity of  $\gamma$ -PGA. It can be assumed that water molecules cannot easily attack the  $\gamma$ -PGA-NP-53 in comparison to  $\gamma$ -PGA. The hydrolysis of the polymer was thus limited by the rate of penetration and diffusion of water into the core of the nanoparticles.<sup>44</sup> Consequently, the hydrolysis ratio of  $\gamma$ -PGA-NP-53 was lower than that of  $\gamma$ -PGA.

**Degradation Behavior of  $\gamma$ -PGA Nanoparticles with  $\gamma$ -GTP.** The enzymatic degradation of  $\gamma$ -PGA nanoparticles was evaluated with  $\gamma$ -GTP.  $\gamma$ -GTP catalyzes the transfer of the  $\gamma$ -glutamyl moiety of  $\gamma$ -glutamyl compounds, such as glutathione, to various amino acids and peptide acceptors.<sup>45</sup> When the acceptor is water, the overall result is hydrolysis. It was observed that the  $\gamma$ -PGA was hydrolyzed to glutamic acids by  $\gamma$ -GTP.<sup>46,47</sup>

In this study, in addition to regular hydrolysis, the enzymatic degradation of  $\gamma$ -PGA,  $\gamma$ -PGA-NP-53,  $\gamma$ -PGA-NP-74, and  $\alpha$ -PGA using  $\gamma$ -GTP was also examined. Four samples of the polymer were used to study the effect of the degree of L-PAE grafting on the degradation or disruption of the nanoparticles with  $\gamma$ -PGA as the main chain. After 2, 4, 6, 12, 24, and 48 h, the degraded samples of the polymer were analyzed by GPC. Figure 3 shows the time dependence of the increased degradation ratio during degradation with  $\gamma$ -GTP. The degradation ratio of  $\gamma$ -PGA and  $\gamma$ -PGA derivatives was found to be dependent on

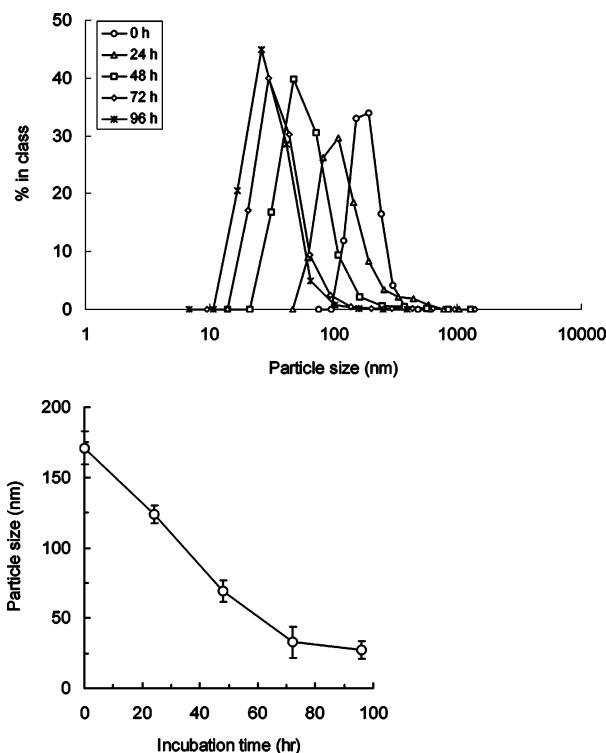


**Figure 4.** Changes in the particle size of  $\gamma$ -PGA nanoparticles prepared from  $\gamma$ -PGA-graft-L-PAE-74 ( $\gamma$ -PGA NP-74) as a function of the degradation time with  $\gamma$ -GTP. The particle size distribution of the  $\gamma$ -PGA nanoparticles was measured in PBS by DLS. The results are presented as means  $\pm$  SD ( $n = 3$ ).

the degradation time. In contrast,  $\alpha$ -PGA was not degraded by  $\gamma$ -GTP. When  $\gamma$ -PGA-NP-53 and  $\gamma$ -PGA-NP-74 were degraded by  $\gamma$ -GTP, the molecular weight of the  $\gamma$ -PGA-graft-L-PAE decreased to about 30% and 20% of the weight prior to degradation.  $\gamma$ -PGA and  $\gamma$ -PGA-NP-53 did not show any significant differences in their degradability after 48 h of incubation with  $\gamma$ -GTP. However, the degradation of  $\gamma$ -PGA-NP-74 was slower than that of  $\gamma$ -PGA. The increased grafting degree of L-PAE may have enhanced the hydrophobic interactions between the L-PAE groups attached to the  $\gamma$ -PGA backbone, resulting in an increased packing and stability of the hydrophobic core. The core of the  $\gamma$ -PGA nanoparticle is formed by a hydrophobic L-PAE and a hydrophilic  $\gamma$ -PGA. Therefore, it is suggested that the  $\gamma$ -PGA incorporated into the core is resistant to degradation by  $\gamma$ -GTP. In general, it is known that enzymatically catalyzed reactions usually require the interaction of several amino acid residues from the substrate with the active site of the enzyme. In the case of  $\gamma$ -PGA nanoparticles, because the hydrophobic L-PAE groups are attached to the  $\gamma$ -PGA backbone, the conformation of  $\gamma$ -PGA-graft-L-PAE is more complex. It has been reported that the rate of enzymatic degradation of a polypeptide and its derivatives was dependent upon the hydrophobicity, D/L isomer composition, conformation ( $\alpha$ -helix and random coil), and modifications of the side chain of polymer.<sup>48–51</sup> Moreover, there was no difference in the degradability of  $\gamma$ -PGA versus  $\gamma$ -PGA-NP-53 using  $\gamma$ -GTP. This difference may be due to the nature of the enzyme used. These results suggest that  $\gamma$ -PGA nanoparticles were recognized by  $\gamma$ -GTP and degraded despite the hydrophobic amino acid modifications.

The change in the particle size of  $\gamma$ -PGA-NP-74 as the degradation progressed with  $\gamma$ -GTP is shown in Figure 4. The particle size of the nanoparticles decreased gradually upon increasing the degradation time.  $\gamma$ -PGA nanoparticles in a buffer

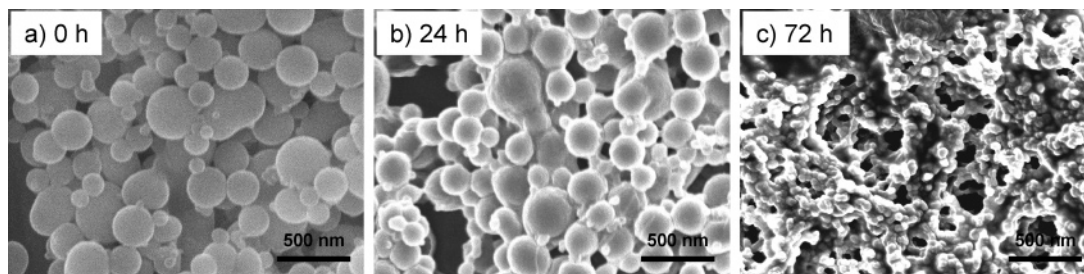


**Figure 5.** SEM images of  $\gamma$ -PGA nanoparticles ( $\gamma$ -PGA NP-74) following enzymatic degradation with  $\gamma$ -GTP. (a) Before degradation, (b) after 24 h of degradation, and (c) after 72 h of degradation.

solution without  $\gamma$ -GTP are stable over several days, with no significant changes in particle size or distribution (data not shown). This result is consistent with the decrease in the molecular weight of  $\gamma$ -PGA-*graft*-L-PAE. This decrease in the particle size probably occurred upon the dissociation of the degradation products from the nanoparticles. Moreover, it is suggested that the molecular weight of the  $\gamma$ -PGA as a main chain is related to the formation of these nanoparticles.

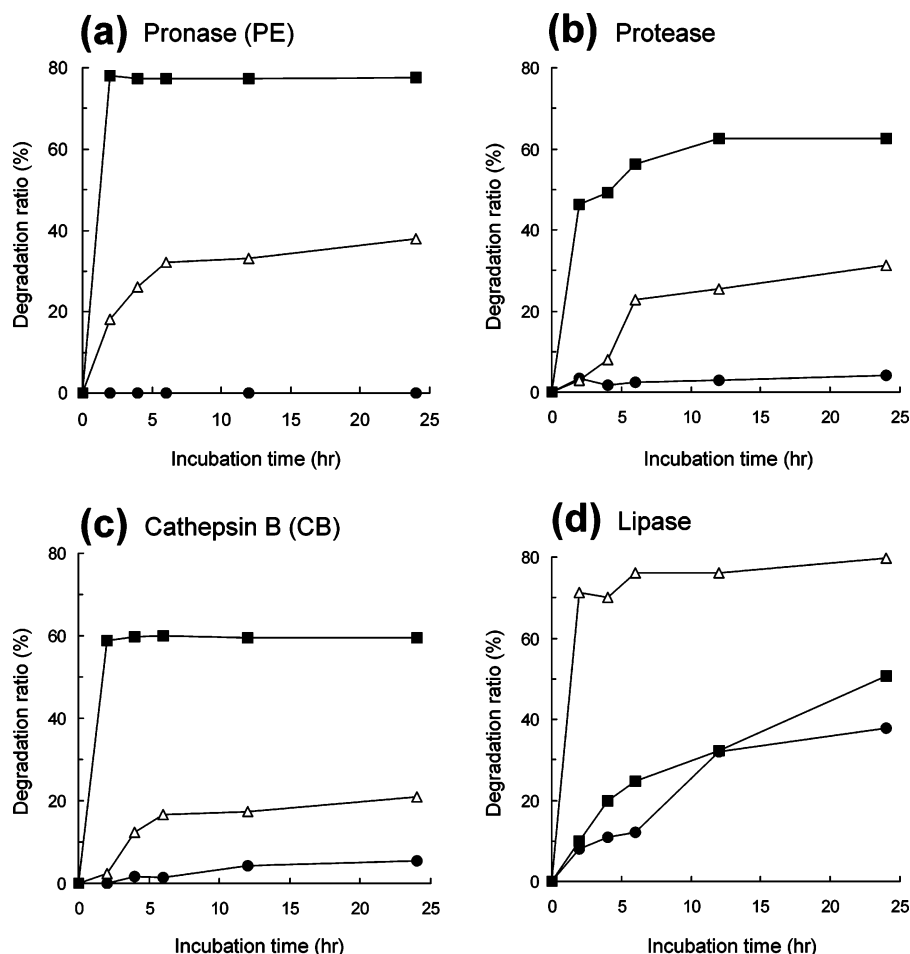
Figure 5 shows the time-course of the changes in the morphology of  $\gamma$ -PGA-NP-74 following incubation with  $\gamma$ -GTP. Prior to the enzymatic degradation, the  $\gamma$ -PGA nanoparticles were spherical with a diameter ranging from <100 to 400 nm. The particle size obtained from the SEM image was different from the DLS data. This difference can be attributed to change in particle size between the dried and hydrated states. In the case of SEM, the SEM image represents the particle size in a dried sample, whereas the DLS method entails measurement of the particle size in a hydrated state. The particle size of  $\gamma$ -PGA-NP-74 showed a broad size distribution for the dried state of the sample. Following degradation for 24 h, the morphologies of the nanoparticles became irregular, and their spherical shape was gradually lost. After 72 h, the particle size decreased dramatically. With further degradation, the nanoparticles disappeared completely. After enzymatic degradation, the  $\gamma$ -PGA nanoparticle solution became transparent. In contrast,  $\gamma$ -PGA-NP-53 was disrupted by degradation with  $\gamma$ -GTP for 6 h (data not shown). These results indicated that the disruption of nanoparticles could be regulated from hours to days by controlling the degree of L-PAE grafting.

**Enzymatic Degradation of  $\gamma$ -PGA Nanoparticles.** Four enzymes [Pronase E (PE), protease from *Aspergillus sojae* (protease), cathepsin B (CB), and lipase] were selected for the enzymatic degradation of  $\gamma$ -PGA,  $\gamma$ -PGA-NP-53, and  $\alpha$ -PGA. Three samples of polymer were used to study the cleavage of the amide bond between the  $\alpha$ -carboxylate side chain of  $\gamma$ -PGA and L-PAE. PE is a serine protease complex derived from bacteria. CB belongs to the family of cysteine proteases and has been found in various cells. It is involved in the intracellular digestion of extracellular proteins taken in by endocytosis. The enzymatic degradation studies were carried out in vitro at 37 °C in PB containing each enzyme. Figure 6 shows the degradation ratio after enzymatic degradation for 0, 2, 4, 6, 12, and 24 h with PE (a), protease (b), CB (c), and lipase (d).  $\gamma$ -PGA-NP-53 and  $\alpha$ -PGA were degraded by these four enzymes into different degradation patterns.  $\alpha$ -PGA was degraded rapidly by PE, protease, and CB but slowly by lipase. Using PE, protease, and CB, the degradation rate was rapid, with 50–80% degradation after less than 2 h. In contrast,  $\gamma$ -PGA was only affected by lipase. It has been reported that  $\gamma$ -PGA could not be easily degraded by proteases, such as papain, pepsin, and bromelain.<sup>52,53</sup> In the case of  $\gamma$ -PGA-NP-53, a decrease of molecular weight in the  $\gamma$ -PGA-*graft*-L-PAE was observed with all enzymes tested. Different enzymes lead to distinct changes

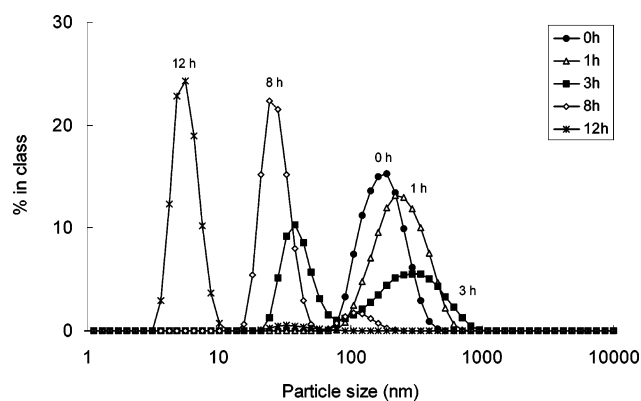
in the degradation ratio of  $\gamma$ -PGA-NP-53. After 24 h of incubation, degradation ratios of 38%, 31%, 21%, and 76% were observed for PE, protease, CB, and lipase, respectively. There are two possible cleavage sites on  $\gamma$ -PGA-*graft*-L-PAE. One is the amide bond of the  $\gamma$ -PGA composed of  $\gamma$ -linked glutamic acids, and the other is the amide bond between the  $\alpha$ -carboxylate side chains of the  $\gamma$ -PGA and L-PAE. When the L-PAE introduced into  $\gamma$ -PGA is cleaved completely, the molecular weight decreases by about 50%. From Figure 6, it can be seen that the cleavage of  $\gamma$ -PGA occurred with lipase, and the cleavage of the amide bond between the  $\alpha$ -carboxylate side chains of  $\gamma$ -PGA and L-PAE occurred using PE, protease, CB, and lipase.

Figure 7 shows the change in the particle size of  $\gamma$ -PGA-NP-53 as the degradation progressed with PE. The size of the nanoparticles increased slightly from 190 to 257 nm during the first 1 h and then gradually decreased with time. After 3, 8, and 12 h, the size of the nanoparticles was about (310, 40 nm), (120, 30 nm), and 6 nm, respectively. After 3 h of degradation, the histogram obtained from the DLS measurements showed a bimodal size distribution. In our previous study, we demonstrated that the size of the  $\gamma$ -PGA nanoparticles increased with a decreasing degree of L-PAE grafting.<sup>32</sup> The increased grafting degree enhances the hydrophobic interactions between the L-PAE groups attached to the  $\gamma$ -PGA backbone, resulting in an increased stability of the hydrophobic cores. These results suggest that the enzymatic cleavage of L-PAE may lead to a looser parking of the core of the nanoparticles. Therefore, the increase in the particle size at the initial degradation may be attributed to an increase in the swelling capacity due to the cleavage of L-PAE in the core of the nanoparticles. On the other hand, the hydrophobic interactions of L-PAE attached to  $\gamma$ -PGA were significantly reduced with increasing degradation time and is not sufficient to form nanoparticles. Therefore, the decrease in the particle size with further degradation probably occurs upon the dissociation of the  $\gamma$ -PGA-*graft*-L-PAE from the nanoparticles, or via the aggregation of  $\gamma$ -PGA-*graft*-L-PAE detached from the nanoparticles. It is suggested that the bimodal size distribution at after 3 h of degradation was due to the increase in the swelling capacity due to the cleavage of L-PAE and the dissociation of the  $\gamma$ -PGA-*graft*-L-PAE from the nanoparticles. These results indicated that, during the degradation process, the size of the  $\gamma$ -PGA nanoparticles changed significantly. It has also been reported that the hydrolytic degradation of amphiphilic block copolymer micelles affected their particle size and morphologies.<sup>54</sup>

**Detection of the Degradation Products of the  $\gamma$ -PGA Nanoparticles.** The detection of the degradation products of  $\gamma$ -PGA-NP-53 with PE was performed by assaying the amino acids using the ninhydrin assay. After 12 h of degradation, the amount of degraded amino acids represented 23% of the initial feeding amount of  $\gamma$ -PGA-NP-53. In contrast, the degradation ratio of  $\gamma$ -PGA and  $\alpha$ -PGA obtained from the ninhydrin assay



**Figure 6.** Enzymatic degradation of  $\gamma$ -PGA,  $\gamma$ -PGA nanoparticles ( $\gamma$ -PGA NP-53) and  $\alpha$ -PGA by Pronase E (PE) (a), protease from *Aspergillus sojae* (protease) (b), cathepsin B (CB) (c), and lipase (d) for different incubation periods at 37 °C. (●) Unmodified  $\gamma$ -PGA, (Δ)  $\gamma$ -PGA-graft-L-PAE-53 ( $\gamma$ -PGA NP-53), and (■)  $\alpha$ -PGA. The degradation ratio was calculated as  $[(M_{n0} - M_{nt})/M_{n0}] \times 100$ , where  $M_{n0}$  and  $M_{nt}$  are the number-averaged molecular weight prior to degradation and the  $M_n$  at "t" time of degradation, respectively. The results represent the average mean from two separate experiments.



**Figure 7.** Changes in the particle size of  $\gamma$ -PGA NP-53 as a function of the degradation time with Pronase E (PE). The particle size distribution of the  $\gamma$ -PGA nanoparticles was measured in PBS by DLS.

was 1.1% and 31%, respectively. The degradation of  $\gamma$ -PGA-NP-53 with PE was also analyzed by  $^1\text{H}$  NMR to determine the cleavage sites and to detect the changes in the chemical structure of  $\gamma$ -PGA-graft-L-PAE. There were no new peaks appearing on the NMR spectrum between the untreated  $\gamma$ -PGA-NP-53 and the sample degraded with PE (data not shown). However, for the sample that was degraded for 12 h, the degree of grafting of L-PAE decreased from 53% to 30%. These results are in agreement with the degradation ratio determined from the ninhydrin assay.

## Conclusion

Amphiphilic graft copolymers composed of  $\gamma$ -PGA as the hydrophilic backbone and L-PAE as the hydrophobic segment were successfully synthesized by grafting L-PAE onto  $\gamma$ -PGA using water-soluble carbodiimide. Due to their amphiphilic properties, the  $\gamma$ -PGA-graft-L-PAE copolymers were able to form nanoparticles. The hydrolytic degradation rate of  $\gamma$ -PGA and  $\gamma$ -PGA hydrophobic derivatives depended on the hydrophobicity of the polymer. Furthermore, we confirmed that the  $\gamma$ -PGA nanoparticles could be degraded and collapsed by various enzymes. The enzymatic digestion of the nanoparticles occurred via the degradation of  $\gamma$ -PGA as the main chain and L-PAE as the side chain. The degradation of the  $\gamma$ -PGA backbone by  $\gamma$ -GTP resulted in a dramatic change in nanoparticle morphology. With increasing time, the  $\gamma$ -PGA nanoparticles reduced in size, and finally disappeared completely. The biodegradability of the  $\gamma$ -PGA nanoparticles was further confirmed by enzymatic degradation with four enzymes (PE, protease, CB, and lipase). All of the enzymes tested were able to cleave the amide bond between the  $\alpha$ -carboxylate side chains of the  $\gamma$ -PGA and L-PAE. It is expected that biodegradable  $\gamma$ -PGA nanoparticles could encapsulate and immobilize proteins, peptides, plasmid DNA, and drugs. These nanoparticles have great potential as carriers for drug delivery systems. Further studies on its applications are in progress to determine whether

vaccination with antigen-immobilized biodegradable  $\gamma$ -PGA nanoparticles can induce cellular and/or humoral immunity.

**Acknowledgment.** This work was supported by CREST from the Japan Science and Technology Agency (JST).

## References and Notes

- Panyam, J.; Labhasetwar, J. *Adv. Drug Delivery Rev.* **2003**, *55*, 329–347.
- Zhang, L.; Eisenberg, A. *Science* **1995**, *268*, 1728–1731.
- Zhang, W.; Shi, L.; An, Y.; Shen, X.; Guo, Y.; Gao, L.; Liu, Z.; He, B. *Langmuir* **2003**, *19*, 6026–6031.
- Wang, W.; Qu, X.; Gray, A. I.; Tetley, L.; Uchegbu, I. F. *Macromolecules* **2004**, *37*, 9114–9122.
- Lemoine, D.; Francois, C.; Kedzierewicz, F.; Preat, V.; Hoffman, M.; Maincent, P. *Biomaterials* **1996**, *17*, 2191–2197.
- Hans, M. L.; Lowman, A. M. *Curr. Opin. Solid State Mater. Sci.* **2002**, *6*, 319–327.
- Kim, S. Y.; Shin, G.; Lee, Y. M. *J. Controlled Release* **1998**, *56*, 197–208.
- Iijima, M.; Nagasaki, Y.; Okada, T.; Kato, M.; Kataoka, K. *Macromolecules* **1999**, *32*, 1140–1146.
- Kim, S. Y.; Lee, Y. M.; Kang, J. S. *J. Biomed. Mater. Res.* **2005**, *74A*, 581–590.
- Kim, S. Y.; Shin, I. G.; Lee, Y. M.; Cho, C. S.; Sung, Y. K. *J. Controlled Release* **1998**, *51*, 13–22.
- Allen, C.; Yu, Y.; Maysinger, D.; Eisenberg, A. *Bioconjug. Chem.* **1998**, *9*, 564–572.
- Allen, C.; Han, J.; Yu, Y.; Maysinger, D.; Eisenberg, A. *J. Controlled Release* **2000**, *63*, 275–286.
- O'Hagan, D. T.; Jeffery, H.; Davis, S. S. *Int. J. Pharm.* **1994**, *103*, 37–45.
- Li, X.; Deng, X.; Yuan, M.; Xiong, C.; Huang, Z.; Zhang, Y.; Jia, W. *J. Appl. Polym. Sci.* **2000**, *78*, 140–148.
- Liggins, R. T.; Burt, H. M. *Int. J. Pharm.* **2001**, *222*, 19–33.
- Zhang, Y.; Zhuo, R. *Biomaterials* **2005**, *26*, 6736–6742.
- Wu, C.; Gan, Z. *Polymer* **1998**, *39*, 4429–4431.
- Gan, Z.; Jim, T. F.; Li, M.; Yuer, Z.; Wang, S.; Wu, C. *Macromolecules* **1999**, *32*, 590–594.
- Nie, T.; Zhao, Y.; Xie, Z.; Wu, C. *Macromolecules* **2003**, *36*, 8825–8829.
- Xiong, X. Y.; Gan, L. H.; Tam, K. C. *Macromolecules* **2003**, *36*, 9979–9985.
- Xiong, X. Y.; Gan, L. H.; Tam, K. C. *Macromolecules* **2004**, *37*, 3425–3430.
- Akashi, M.; Kirikihara, I.; Miyauchi, N. *Angew. Makromol. Chem.* **1985**, *132*, 81–89.
- Chen, M. Q.; Serizawa, T.; Kishida, A.; Akashi, M. *J. Polym. Sci. A: Polym. Chem.* **1999**, *37*, 2155–2166.
- Sakuma, S.; Suzuki, N.; Kikuchi, H.; Hiwatari, K.; Arikawa, K.; Kishida, A.; Akashi, M. *Int. J. Pharm.* **1997**, *149*, 93–106.
- Akashi, M.; Niikawa, T.; Serizawa, T.; Hayakawa, T.; Baba, M. *Bioconjug. Chem.* **1998**, *9*, 50–53.
- Akagi, T.; Kawamura, M.; Ueno, M.; Hiraishi, K.; Adachi, M.; Serizawa, T.; Akashi, M.; Baba, M. *J. Med. Virol.* **2003**, *69*, 163–172.
- Miyake, A.; Akagi, T.; Enose, Y.; Ueno, M.; Kawamura, M.; Horiuchi, R.; Hiraishi, K.; Adachi, M.; Serizawa, T.; Narayan, O.; Akashi, M.; Baba, M.; Hayami, M. *J. Med. Virol.* **2004**, *73*, 368–377.
- Wang, X.; Uto, T.; Sato, K.; Ide, K.; Akagi, T.; Okamoto, M.; Kaneko, T.; Akashi, M.; Baba, M. *Immunol. Lett.* **2005**, *98*, 123–130.
- Kawamura, M.; Wang, X.; Uto, T.; Sato, K.; Ueno, M.; Akagi, T.; Hiraishi, K.; Matsuyama, T.; Akashi, M.; Baba, M. *J. Med. Virol.* **2005**, *76*, 7–15.
- Matsusaki, M.; Hiwatari, K.; Higashi, M.; Kaneko, T.; Akashi, M. *Chem. Lett.* **2004**, *33*, 398–399.
- Kaneko, T.; Higashi, M.; Matsusaki, M.; Akagi, T.; Akashi, M. *Chem. Mater.* **2005**, *17*, 2484–2486.
- Akagi, T.; Higashi, M.; Kaneko, T.; Kida, T.; Akashi, M. *Macromol. Biosci.* **2005**, *5*, 598–602.
- Akagi, T.; Kaneko, T.; Kida, T.; Akashi, M. *J. Controlled Release* in press.
- Kishida, A.; Murakami, K.; Goto, H.; Akashi, M.; Kubota, H.; Endo, T. *J. Bioact. Compat. Polym.* **1998**, *13*, 270–278.
- Matsusaki, M.; Serizawa, T.; Kishida, A.; Akashi, M. *J. Biomed. Mater. Res. Part A*, **2005**, *73A*, 485–491.
- Shimokuri, T.; Kaneko, T.; Akashi, M. *J. Polym. Sci. A Polym. Chem.* **2004**, *42*, 4492–4501.
- Akiyoshi, K.; Deguchi, S.; Moriguchi, N.; Yamaguchi, S.; Sunamoto, J. *Macromolecules* **1993**, *26*, 3062–3068.
- Wang, W.; Tetley, L.; Uchegbu, I. F. *Langmuir* **2000**, *16*, 7859–7866.
- Guan, H.; Xie, Z.; Zhang, P.; Deng, C.; Chen, X.; Jing, X. *Biomacromolecules* **2005**, *6*, 1954–1960.
- Arimura, H.; Ohya, Y.; Ouchi, T. *Biomacromolecules* **2005**, *6*, 720–725.
- Fan, K.; Gonzales, D.; Sevoian, M. *J. Environ. Polym. Degrad.* **1996**, *4*, 253–260.
- Goto, A.; Kunioka, M. *Biosci. Biotechnol. Biochem.* **1992**, *56*, 1031–1035.
- Kubota, H.; Nanbu, Y.; Endo, T. *J. Polym. Sci. A Polym. Chem.* **1996**, *34*, 1347–1351.
- Martinez Barbosa, M. E.; Cammas, S.; Appel, M.; Ponchel, G. *Biomacromolecules* **2004**, *5*, 137–143.
- Inoue, M.; Hiratake, J.; Suzuki, H.; Kumagai, H.; Sakata, K. *Biochemistry* **2000**, *39*, 7764–7771.
- Abe, K.; Ito, Y.; Ohmachi, T.; Asada, Y. *Biosci. Biotech. Biochem.* **1997**, *61*, 1621–1625.
- Kimura, K.; Tran, L.-S. P.; Uchida, I.; Itou, Y. *Microbiology* **2004**, *150*, 4115–4123.
- Hayashi, T.; Nakanishi, E.; Iizuka, Y.; Oya, M.; Iwatsuki, M. *Eur. Polym. J.* **1995**, *31*, 453–458.
- Chiu, H.-C.; Kopeckova, P.; Deshmane S. S.; Kopecek, J. *J. Biomed. Mater. Res.* **1997**, *34*, 381–392.
- Rypacek, F. *Polym. Degrad. Stab.* **1998**, *59*, 345–351.
- Li, C. *Adv. Drug Deliv. Rev.* **2002**, *54*, 695–713.
- Weber, J. *J. Biol. Chem.* **1990**, *265*, 9664–9668.
- Obst, M.; Steinbuechel, A. *Biomacromolecules* **2004**, *5*, 1166–1176.
- Hu, Y.; Zhang, L.; Cao, Y.; Ge, H.; Jiang, X.; Yang, C. *Biomacromolecules* **2004**, *5*, 1756–1762.

BM050657I